Jordanian Journal of Computers and Information Technology (JJCIT), Vol. 11, No. 04, December 2025.

ENHANCING PALMPRINT RECOGNITION: A NOVEL CUSTOMIZED LOOCV-DRIVEN SIAMESE DEEP-LEARNING NETWORK

Wafaa Mohammed Cherif[1], Javier Garrigós[2], Juan Zapata[2] and Tarik Boudghene Stambouli[1]

(Received: 14-Jul.-2025, Revised: 17-Oct.-2025 and 29-Oct.-2025, Accepted: 29-Oct.-2025)

ABSTRACT

The advancement of deep learning in biometric systems, in which face and hand modalities have been widely implemented, leads to significant improvements in terms of speed performance and data confidentiality. Palmprint recognition is the main focus of the proposed approach, which deals with databases that are relatively smaller than other biometric datasets. A large and complex deep-learning model may overfit and lose its ability to generalize when applied to such data. This study addresses this challenge by implementing a deep learning model suitable for palmprints, which are characterized by diversity and limited data. Initially, the appropriate Region of Interest (ROI) is extracted using active segmentation, which is fitting for dealing with the difficulty of obtaining palmprints from hand images with closely spaced or connected fingers. In the second stage, a novel customized LOOCV Leave-One-Out Cross Validation (A Modified-LOOCV) technique is integrated with a Siamese deep-learning network for palmprint verification. Unlike conventional LOOCV, our modified scheme optimizes the computational cost while achieving a balanced evaluation on three different datasets. The proposed framework rivals the effectiveness of the advanced palmprint-recognition systems with a high recognition accuracy of 99.75%, improved equal error rate (EER), reduced to 0.002, and faster matching time, making it highly suitable for field application.

KEYWORDS

Palmprint recognition, Deep learning, Customized LOOCV, Siamese network.

1. INTRODUCTION

The technology advancements led to identity verification being an absolute necessity and a crucial requirement for user authentication in private and public organizations with rising safety issues and the overlapping user information in order to preserve data and guarantee information security. In the vast majority of identity applications, biometrics, including signatures, fingerprints, iris patterns, faces, and palmprints, currently replaces traditional technologies [1]. In these, palmprint modality advanced to be widely implemented due to its significant individual variation, ease of use even with low-resolution hand images, and high recognition accuracy [2]. Traditional biometric recognition systems relied heavily on unique features created specifically for a given kind of data. A lot of these features rely on transforms like Gabor, Fourier, and wavelet [3], or on edge distribution as Histogram of Oriented Gradients (HOG), Scale-Invariant Feature Transform (SIFT) descriptors, and principal-component analysis (PCA) to minimize the number of feature dimensions [4][5]. These conventional approaches have a number of challenges, such as their inability to handle huge and diverse datasets and their dependence on field knowledge for feature extraction. Deep-learning algorithms have evolved as a solution to these issues, including automatic feature extraction and the capacity to generate hierarchical representations from unprocessed data [6].

For biometrics, deep learning enhances the performance of all recognition systems, increasing their efficiency and the ability to adapt to a wide range of identification challenges [7][8]. These advancements have considerably contributed to palmprint recognition. Compared to fingerprints, palmprints have more creases and have the potential to be used for a more precise representation of identity [9]. Deep learning-based palmprint recognition has been widely investigated; much work on the potential of convolutional neural network (CNN)-based pattern and palmprint recognition has been

1. W. M. Cherif and T. B. Stambouli are with Signals and Images Laboratory (LSI), University of Sciences and Technology Mohamed Boudiaf USTO-MB, BP1505, El M'naouer Oran, Oran, 31000, Algeria. Emails: wafaa.mohammedcherif@univ-usto.dz and bs_tarik@yahoo.com.
2. J. Garrigós and J. Zapata are with Dpto. Electrónica, Tecnología de Computadoras y Proyectos, Universidad Politécnica de Cartagena, Cartagena, 30202, Spain. Emails: javier.garrigos@upct.es and juan.zapata@upct.es.

carried out; however, some crucial issues with overfitting and class imbalance still exist [10]. Similarly, a large database with an important number of images is necessary for CNN and additional deep-learning algorithms. In particular scenarios, like palmprint or fingerprint identification, having a limited number of samples requires protocols to address this insufficient data, including data augmentation, which brings challenges related to modification of the appropriate learning position. As a result, systems that use these processes typically fail to produce accurate results. To deal with these limitations, deep Siamese networks have been proposed to enhance feature extraction and matching processes [11], thus resolving the challenges of standard CNNs for palmprint recognition. Siamese neural networks, contrasted with the CNN algorithms, are built on a Siamese framework that consists of two identical CNNs. The capacity to perform tasks, such as few-shot learning, or learning without new data, is improved by this architecture, which helps learn a distance function that converts the input data into a feature space [12]. The implementation of contrastive loss functions and knowledge transfer learning leads to this increased efficiency and enhances overall system performance. Even with a small number of labeled samples, Siamese networks perform well. This ability is critical in situations when it is challenging to gather large datasets of labeled images using similarity metric learning. Siamese networks may effectively generalize to new classes with a small number of labeled examples or even just one [13]. Through the sharing of weights within sibling networks, Siamese networks perform better than traditional CNNs in terms of resistance to overfitting. This sharing of weights reduces overfitting concerns by improving the model's ability to generalize to new samples.

The potential of Siamese deep networks has been demonstrated in a wide range of applications, including audio classification, time-series analysis, face and palmprint recognition [14][15][16]. It has the ability to avoid overfitting, learn from sparsely labeled data, and improve overall model performance with its reliance on pairwise network learning. However, they have certain limitations due to their requirement for additional computational resources and a longer training time than traditional convolutional neural networks. This study aims to address these limitations by applying a Siamese deep-learning network combined with a Modified Leave-One-Out Cross-Validation (LOOCV) for palmprint recognition. The goal is to overcome challenges related to long training time, hardware requirements, and weak generalization, while enabling rapid and reliable predictions for real-world use. Our model is designed to learn effectively from small-scale palmprint datasets, without relying on extensive data augmentation, which is often necessary in conventional deep-learning methods. To reduce the bias introduced by random data splitting and to shorten execution time, we propose a Modified LOOCV technique that better utilizes the available samples. The approach is validated on four public palmprint databases of varying quality and class sizes.

The key contributions of this work are summarized as follows:

- Application of a small Siamese deep-learning network specifically designed for the nature of palmprint images, which are highly similar in structure. The model effectively supports few-shot learning, making it suitable for datasets with limited samples. It reduces computational complexity, avoids overfitting on small datasets, enables efficient training with limited resources, and is easy to apply in real-world scenarios without requiring data augmentation or similar techniques.
- Implementation of a novel Modified Leave-One-Out Cross-Validation (LOOCV) technique, which ensures efficient use of all available samples, reduces bias from random splits, and accelerates training while preserving strong generalization.
- Combination of the Siamese architecture with the Modified LOOCV, providing both high recognition accuracy and practical deployment feasibility by lowering training time and hardware requirements.
- Comprehensive evaluation on four public contactless palmprint databases of varying sizes and conditions, demonstrating the robustness, reliability, and generalization ability of the proposed approach compared with state-of-the-art methods.

The remaining content of the paper is organized as follows: Section 2 gives a brief overview of palmprint-recognition systems based on CNN and Siamese networks. The experimental procedures and methodology of our study are described further in the third section. The databases used and the experiment results are shown and discusesed in Section 4. Section 5 presents the final conclusion.

2. RELATED WORKS

A variety of deep-learning networks have been used in research papers that offer palmprint-based identification systems. This section aims to review recent advances in deep learning for palmprint recognition, CNN and Siamese networks, taking advantages of their enhanced feature-extraction expertise to outperform classic methods. Table 1 summarizes the most important networks applied.

A recent study [17] applied various CNN architectures to the Birjand University Mobile Palmprint Database (BMPD) offered by Kaggle, which consists of images taken over two different sessions with different rotations. MobileNet outperformed Xception at 88.3% and VGG16 at 70.8% accuracies, with a score of 96.6%. These outcomes demonstrate the superior efficacy of MobileNet in palmprint recognition when evaluated compared to different alternatives. Considering these results, it can be argued that CNNs have achieved very positive results in most plamprint-recognition systems. Recent research has examined palmprint-recognition systems' reliability and security. Multi-Order Extension Codes (MOECs), which combine first-order (1TFs) and second-order (2TFs) texture features, were initially presented by Liao et al. [18] in order to capture additional discriminative information. By combining these characteristics, their approach outperformed conventional texture-coding methods and consistently improved recognition accuracy across Contact-based, contactless, and multi-spectral palmprint databases, including PolyU and IITD, offering an important conventional reference against which recent CNN-based techniques can be compared. Yan et al. [19], on the other hand, proposed a Generative Adversarial Network GAN-based palmprint reconstruction attack applying a modified Progressive GAN (ProGAN) in order to concentrate on the security aspect. They developed a Scale-Adaptive Multi-Texture Complementarity (SAMTC) loss to improve the realism of reconstructed images and a Double Reuse Training Strategy (DRTS) to maximize learning from sparse data. Their research revealed that existing palmprint systems are susceptible to template reconstruction, posing significant privacy and security issues. Recent work has improved palmprint recognition by addressing concerns with privacy, robustness, and generalization. To solve the problem of mislabeled training data, Shao et al. [20] developed a Multi-Stage Noisy Label Selection and Correction (MNLSC) framework. Their method may increase accuracy by more than 30% under high noise rates. A Federated Metric Learning (FedML) technique was concurrently proposed by Shao et al. [21], which allowed multiple users to train together without disclosing private information. This improved recognition accuracy across 18 datasets while preserving confidentiality. In addition, another research [22] focused on generalizing across datasets, creating techniques including transfer learning and adversarial learning that address domain gaps and improve performance on unknown datasets. These contributions demonstrate the trend toward improving palmprint recognition's accuracy while also making it more resilient to noise, cross-domain adaptable, and privacy-preserving.

Zhang et al. [23] provided an integrated CNN-Transformer Global-Local Gating and Adaptive fusion Network (GLGAnet) palmprint-recognition system that combines the Transformer's global modeling with the CNN's local feature extraction. The framework takes advantage of an adaptive feature fusion module and a gating mechanism, with 98.5% and 99.5% recognition accuracy on the Tongji and Hong Kong Polytechnic University datasets, respectively. To increase the effectiveness of CNN while avoiding some of its drawbacks, specifically when handling small datasets and differentiating between really similar classes, numerous current studies recommend implementing the Siamese networks, which advance in image recognition [24], address the drawbacks of conventional techniques by achieving higher accuracy along with processing efficiency. Marattukalam et al. [25] Introduced a Siamese neural-network design for N-shot palm-vein identification. This architecture was created to address a typical biometric recognition problem. Impressive performance metrics were attained by the network when tested on the HK PolyU multi-spectral palm-vein database: 91.5% F1-score, and 90.5% accuracy. Despite the small amount of data, these results demonstrate the architecture's efficacy and potential for practical biometric applications. A relevant approach by Gurunathan et al. [26] presented a palm-vein biometric system using a Siamese network processing distinctive vein patterns for authentication. Compared to conventional biometrics, this approach has benefits including increased accuracy and resistance to spoofing. It is also computationally efficient for mobile use and adaptive to evolving vein patterns over time.

Zhong et al. [27] proposed a palmprint-recognition technique that extracts convolutional features from palmprint images using a Siamese network with two parameter-sharing VGG-16 networks; the network compares these features to evaluate similarity and recognition accuracy. The approach

showed robustness with an Equal Error Rate (EER) of 4.559% on the XJTU dataset, while it achieved an EER of 0.2819% on the PolyU dataset. These outcomes demonstrate the method's efficacy and versatility across various datasets. In light of these findings, two subsequent studies [28][29] have suggested a Meta-Siamese Network-based palmprint recognition. The initial experiment [28] presented a Meta-Siamese network that uses episodic training to improve feature integration and similarity metrics, building upon the Siamese network architecture. Using deep hashing networks, this model was expanded to zero-shot recognition tasks and showed competitive performance on eight different datasets. In the second experiment [29], a new Meta-Siamese Network (MSN) intended for small-sample palmprint identification was shown. Applying a flexible architecture and two distance-based loss functions to improve optimization, this method used episodic training. The MSN model demonstrated significant improvements over baseline approaches in both confined and unconstrained benchmark palmprint databases. Furthermore, a recent study [16] implemented the Siamese network for palmprint identification that uses two CNNs to extract and compare palmprint features using shared weights. A loss of variance function is used to assess the extracted features and determine whether or not the images are of the same person. The approach demonstrated its efficacy with a 0.044 equal error rate and 95.6% recognition accuracy.

Table 1. A summary of significant previous work based- CNN for palmprints.

Ref/Model	Year	Method	Datasets	Accuracy
[30] Siamese-Hashing Network	(2019)	SHN. A non-pooling Siamese-Hashing Network structure.	PolyU Multi-spectral palm-print dataset	97.98%
[31] InceptionResNet-v2	(2022)	InceptionResnet-v2 pre-trained deep-neural networks (DNNs), with Rectified Linear Unit (ReLU), dropout, and fully connectedWith Soft max.	PolyU palm-print database	99.21%
[32] LeNet-5	(2022)	LeNet-5 Convolutional Neural Network	Tongji Contactless Palm-print Dataset	97%
[16] Siamese Network	(2023)	Siamese Network with a loss of variance function for similarity prediction.	CASIA, THU-PALMLAB	95.6% (EER: 0.044)
[33] Pretrained VGG16 within Siamese Frame-work	(2023)	Siamese network with VGG-16. Palmprint feature extraction is used to determine palmprints' similarity.	CASIA dataset	91.8% (left hand), 91.7% (right hand)
[23] Gating mechanism and adaptive feature fusion	(2023)	Integration of CNN and Transformer-GLGAnet for palmprint recognition.	Tongji U dataset, Hong Kong Polytechnic dataset	98.5%, 99.5%
[17] CNNs	(2024)	Convolutional Neural Network models with the Xception, VGG16, ResNet50, MobileNet, and EfficientNetB0 architectures.	BMPD dataset	96.6%
[34] Fusion Mechanism	(2024)	Fusion Mechanism with Multi-direction Gabor Filter for prediction optimization.	CASIA palm-print database	99.41%

In support of the most important results based on Siamese and CNN networks, our study relies on the Siamese network by integrating a Modified LOOCV for enhancing its findings. In light of these advantages, the proposed approach remains excellent for field implementation, where it provides excellent recognition results, faster speed and less memory usage, which improves palmprint-recognition systems.

3. METHODOLOGY

The proposal focuses on the enhancement of a palmprint-recognition system, consisting of two main stages: pre-processing and palmprint recognition using the Siamese network based on the Modified-LOOCV technique.

Jordanian Journal of Computers and Information Technology (JJCIT), Vol. 11, No. 04, December 2025.

3.1 Pre-processing

In this stage, the Region of Interest (ROI) is extracted, based on active contour segmentation. Our goal is to implement a snake-based model for the segmentation of hand images, with the intention of creating a model that is robust and capable of identifying the hand valley points and correctly extracting the region of interest, thereby addressing the limitations of the traditional methods, which have produced erroneous findings when extracting ROIs from hand images with two conjoined fingers.

The active contour model, often referred to as snakes, has its roots in elastic models but is primarily credited to the pioneering work of the Kass team [35]. These models derive their name from their capacity to deform themselves into snake-like shapes Figure 1.

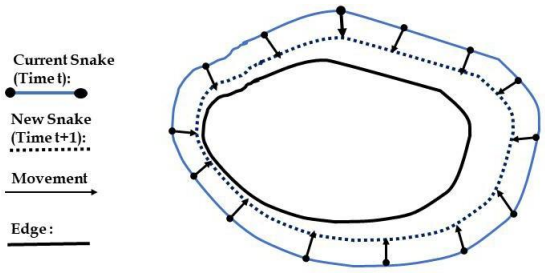

Figure 1. Closed snake active contour model.

Figure 2 demonstrates how the active contour method is applied. The contours are highlighted in red. In our proposed methodology, active contour is employed with the specific goal of precisely delineating the areas between the hand and fingers, particularly in scenarios where the fingers appear to be stuck together or tangled. The method of active contour [32] is based on an initial contour and then concentrates on the contour line that needs to be produced by means of the impact of internal and external energy on a closed snake model. Figure 2a displays the initial contour obtained through Otsu's method. However, this method is not effective for determining edges in small areas (closed fingers).

Subsequently, in Figure 2b the active contour model applies the initial contours obtained as the starting point for active-contour application, successfully extracting contours in limited areas (closed fingers). This process enables the accurate extraction of the Region of Interest (ROI), which defines the core contribution of our suggested pre-processing procedure.

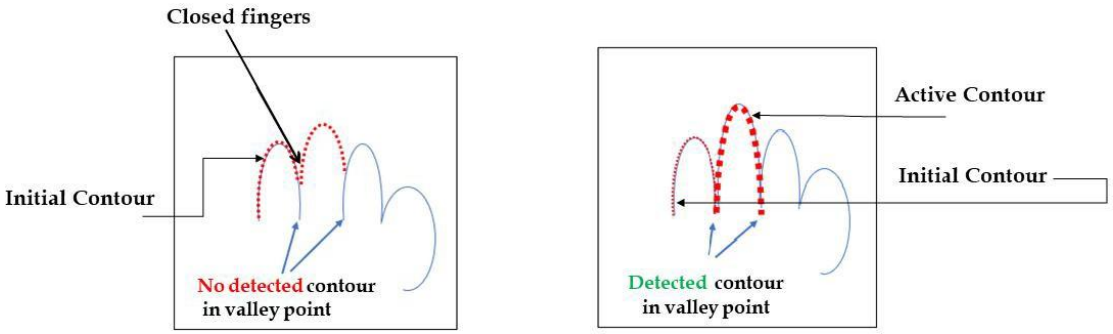

(a) Initial contour based on the threshold method. (b) Final contour based on active-contour segmentation.

Figure 2. Principles of active-contour application.

- **ROI Extraction**

  In the process of Region of Interest (ROI) extraction, several main tasks are involved. Initially, the input color image is converted into grayscale, the background is removed, and the hand contour is extracted using active segmentation. As shown in Figure 3, the hand edge is first extracted (b) and combined with the segmentation mask to preserve structural details (c). Morphological operations are then applied to progressively remove noise and refine the contour (d–e). Since hand images often contain light reflections, these are explicitly detected (f) and integrated into the mask to improve boundary accuracy. The final output (g) provides a clean

hand contour. This sequential refinement ensures robustness by addressing noise and reflections, resulting in a reliable region of interest extraction for the next step.

Figure 4 demonstrates the enhanced performance of the active contour over traditional threshold segmentation, on two original hand images. Due to the limits of the middle and ring fingers (closed fingers), Otsu thresholding, and Kirsch edge detector segmentation in (b) it was unable to identify the entire contour and valley points. Instead, as (c) shows, the active contour model is effective at locating the complete contour (active contour) from the initial contour, especially in the narrow areas between the fingers (closed fingers), which makes it easier to identify and extract the valley points as well as the Region of Interest (ROI) for the next phase. The Valley Points Extraction involves identifying four points corresponding to finger intersections by analyzing local minima through the contour employing a combination of methodologies detailed in [36][37], which provides a comprehensive overview of the process. Finally, ROI Computation computes the ROI based on extracted valley points. Section 4.2 illustrates the details of the final ROI extraction result.

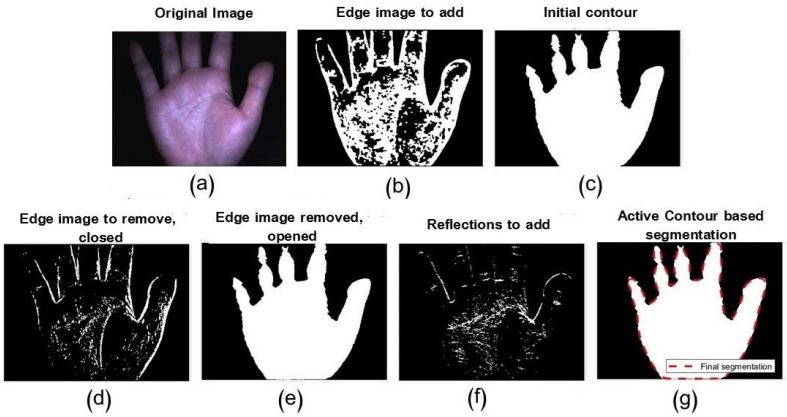

Figure 3. Active-contour hand segmentation: (a) Original image, (b) Edge image to add, (c) Initial contour from Otsu with edge fusion, (d) Edge image to remove (closed), (e) Edge image removed (opened), (f) Reflections to add, and (g) Final active-contour segmentation.

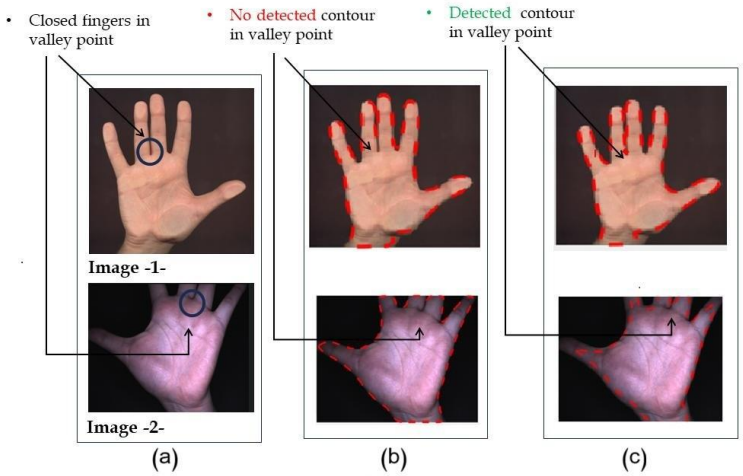

Figure 4. Active-contour application for hand images: (a) Two original images displaying fingers linked together; (b) Threshold segmentation; (c) Active contour-based segmentation.

3.2 Palmprint Recognition: The Modified LOOCV-based Siamese Network

The Leave-One-Out Cross Validation (LOOCV) technique is used to evaluate multiple machine and deep learning-based models. It consists of training the model several times (iterations), by leaving out one image from the entire database, and using the rest of the images for the training phase. This process is repeated depending on the total number of images in the database. The results of all iterations are averaged to get a final model performance. Figure 5 provides the standard LOOCV process, where for each itteration, one sample is left out for testing while the remainder is used for

training. Compared to k-fold, repeated k-fold cross validation, or simple random split algorithms, Leave-One-Out Cross Validation (LOOCV) has several advantages. It generates an estimate of the generalization error that is nearly unbiased, making it a more accurate test than traditional splitting techniques. Experimental comparisons [38] have also demonstrated that, through appropriate parameter tuning, LOOCV can provide higher sensitivity and more balanced accuracy in certain classifiers, including Random Forest and Bagging.

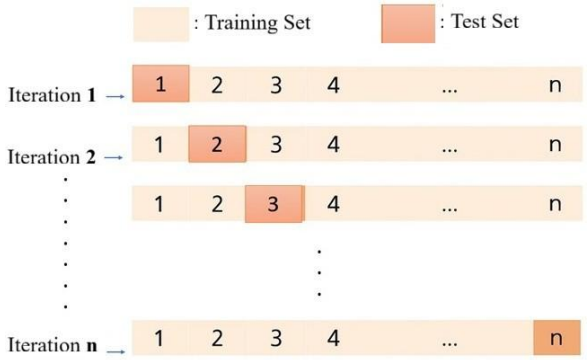

Figure 5. Standard LOOCV (leave-one-out cross validation).

In palmprint recognition, where images show high similarity and datasets are generally smaller, LOOCV provides obvious benefits. Testing each sample reduces the possibility of inaccurate results from random splits and guarantees thorough and objective evaluation. However, due to the high computational demand of LOOCV, we propose a Modified LOOCV to avoid the computational expenses associated with standard LOOCV. Instead of excluding one image from the entire dataset in each iteration, we exclude two images from each class for testing while using the remaining ones for training, as shown in Figure 6. This method involves training the model, as in LOOCV, but then taking the result from the first iteration due to its consistently outstanding performance. Table 2 outlines the distinctions between Standard and Modified LOOCV.

Table 2. Comparison of traditional LOOCV and modified LOOCV.

Aspect	**Traditional LOOCV**	**Modified LOOCV**
In each iteration	Leaves one image out from each class of the entire dataset.	Leaves two images from each class of the entire dataset.
Performance-assessment	Requires completion of all iterations to fully assess model performance.	Allows rapid evaluation from the first iteration.
Deployment-efficiency	Prolongs model deployment due to iterative training and evaluation.	Demonstrates practical performance for real-world applications-evaluation from the first iteration.

For instance, in a dataset with 600 classes and 10 images per class, leaving out 2 images per class for testing in the first iteration allows for a thorough evaluation: 1200 images in testing (20% of the dataset) and 4800 in training (80%).

Unlike random selection methods, as the train-test-split validation, the Modified LOOCV ensures that all classes are represented in the testing data, enhancing evaluation reliability. Moreover, it yields comparable accuracy to standard LOOCV, but with reduced computational complexity, optimizing efficiency without compromising performance assessment. The Modified LOOCV is integrated into the training process of the Siamese network, as illustrated in Figure 6.

Before initiating the LOOCV loop, the main database is divided into several classes, each representing a person with a unique label and containing ten image samples. This ensures that at least two samples per class are available for testing, maintaining class balance across iterations.

The Siamese network is then trained using the Modified Leave-One-Out Cross Validation strategy. In this setup, two identical sub-networks process paired inputs to assess their similarity. The architecture of the Siamese model, illustrated in Figure 7, consists of twin branches that share the same weights, allowing both inputs to be transformed through identical feature-extraction operations. This shared-weight mechanism ensures consistent feature representation and enhances the model's ability to distinguish between genuine and impostor pairs.

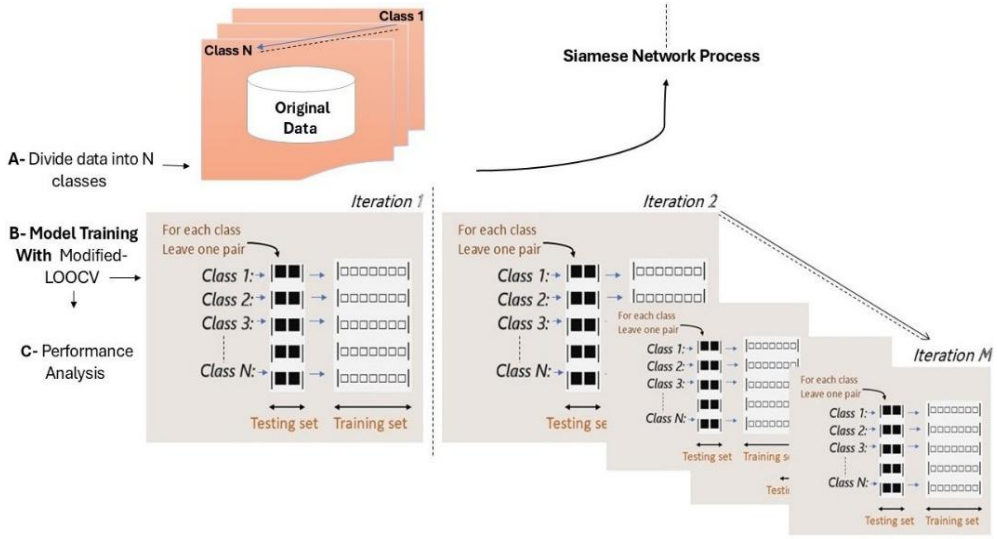

Figure 6. Modified LOOCV workflow.

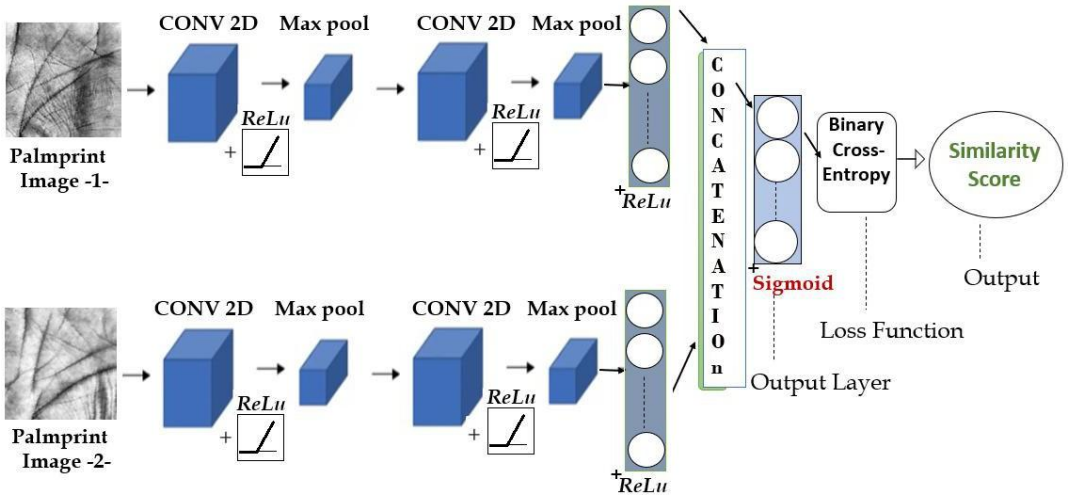

Figure 7. Siamese-network architecture.

The Siamese-network architecture includes two main components:

1) **Principal Network:** This component processes input palmprint images and extracts discriminative features through convolutional and fully connected layers. The detailed configuration is presented in Table 3. The first convolutional layer (Conv1) employs a large kernel of 10×10 with 64 filters and a stride of 1 to capture global edges and texture patterns, minimizing the need for deeper networks. The second convolutional layer (Conv2) applies a smaller 7×7 kernel to refine local structures. Each convolutional block is followed by a max pooling layer that reduces spatial dimensions and strengthens invariance. The fully connected layer (4096 neurons) transforms the extracted maps into compact embeddings suitable for comparison. This architecture effectively prevents overfitting on small palmprint datasets while maintaining low computational cost, making it highly suitable for real-time biometric applications.

2) **Similarity Metric:** After feature extraction, the similarity between embeddings is computed using a metric defined in Equation 1. The resulting values are passed through a sigmoid activation function (Equation 2), producing probabilities that express the degree of similarity between pairs of samples. Higher probabilities indicate greater similarity, while lower ones indicate dissimilarity.

$$\text{Similarity Scores} = \sigma(\text{output}) \tag{1}$$

where:

Similarity Scores: Output probabilities representing the similarity between input pairs.

$\sigma(x)$**:** Sigmoid function is defined as:

$$\sigma(x) = \frac{1}{1+e^{-x}} \tag{2}$$

Table 3. Siamese-network parameters.

Layer	Feature Map	Size	Kernel Size	Stride
Input image	1	150x150	-	-
CONV1	64	141x141	10x10	1
Max Pool	64	70x70	2x2	2
CONV2	128	64x64	7x7	1
Max Pool	128	32x32	2x2	2
FC1	4096	1x1	-	-
Output	1	1x1	-	-

Outputs: The feature similarity scores generated by the Siamese network.

To optimize the model, the Binary Cross-Entropy (BCE) loss function is used, as shown in Equation 3. This function efficiently drives the network to produce closer embeddings for similar pairs and distant ones for dissimilar pairs, thus improving discriminative capability.

$$L = [y.\log(p) + (1-y).\log(1-p)] \tag{3}$$

Here, L represents the computed loss for each pair, y is the ground-truth label (1 for similar, 0 for dissimilar), and p denotes the predicted probability of similarity. During training, the network minimizes this loss through gradient-based optimization to generate robust and discriminative feature embeddings.

For each Modified-LOOCV iteration, independent datasets are formed for training and testing, ensuring that all classes contribute representative samples. The Siamese network is initialized with its optimizer and trained for several epochs using the BCE loss. After training, performance is evaluated based on accuracy and Equal Error Rate (EER). Additionally, loss, accuracy, and ROC curves are plotted to visualize the trade-off between true and false positive rates at different thresholds.

The proposed Siamese network integrated with the Modified LOOCV and optimized *via* Binary Cross-entropy loss provides an effective framework for palmprint recognition. It offers precise similarity measurement between paired samples while maintaining high efficiency and strong generalization across datasets.

4. RESULTS AND DISCUSSION

4.1 Datasets and Experimental Environment

To demonstrate our segmentation method and evaluate the recognition accuracy of the proposed method, we considered the four contactless databases, three were employed for model training, and the fourth was kept unseen during training to serve as an independent dataset for prediction and evaluation. Some typical samples from the employed palmprint databases are illustrated in Figure 8. The Tongji Contactless Palmprint Database, developed at Tongji University in China with a dedicated acquisition device, includes images from 600 subjects captured over two sessions [39][40]. The IIT Delhi Touchless Palmprint Database (V1.0) IITD [41][42], contained color images with various artifacts and illumination changes. The GPDS150 Palmprint Database, created in Spain, provides palmprint images from 150 individuals, adding further variability in acquisition settings and subject diversity [43]. the PolyU DB (Version 2.0) [44]includes 1140 right-hand (2D and 3D) images taken of 114 individuals. To enable for evaluation under different position settings, each participant presented five contactless hand poses in various orientations. The most important characteristics of these databases are summarized in Table 4.

The proposed ROI extraction process is demonstrated in MATLAB R2018a, and the palmprint-recognition model is trained in Python within an Anaconda environment on Ubuntu. The experiment includes an Intel Core i9-9820X (LGA-2066), 64 GB DDR4 RAM (4×16 GB Ballistix Sport LT, 2400 MHz) and Nvidia RTX 2080 Ti GAMING OC 11 GB GPUs (TU102, Rev. A).

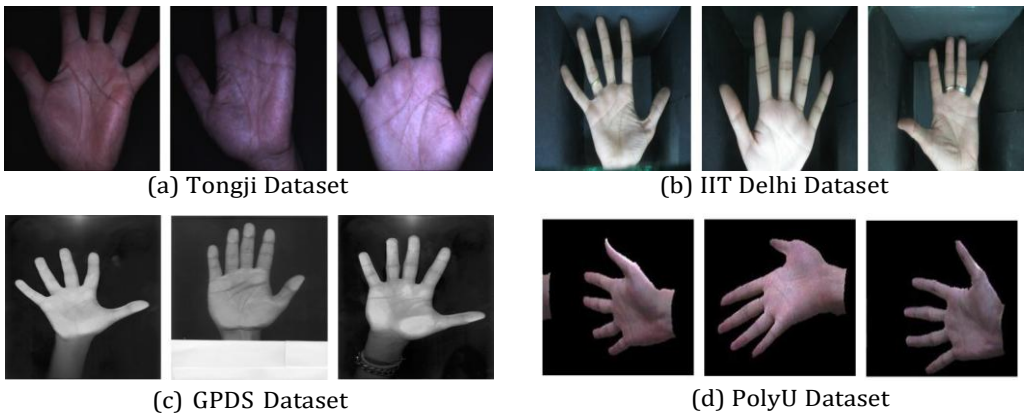

Figure 8. Typical samples from the palmprint datasets: (a) Tongji, (b) IIT Delhi (V1.0), (c) GPDS, and (d) PolyU DB (Version 2.0).

Table 4. Databases' characteristics.

Details	Tongji DB	IITD DB	GPDS DB	PolyU DB
Number of	600	230	150	114
Number of	10	5	10	5
Number of images Gray/color	6000 Gray scale	1265 Gray scale	1500 Gray scale	1140 (2D + 3D) Color (2D) + 3D depth
Resolution devices	800 × 600 Camera	800 × 600 Camera	1403 × 1021 HP Scanner	640 × 480 Minolta VIVID 910 3D digitizer
Origin	Chinese	Indian	Spanish	Hong Kong (zPolyU)

4.2 ROI Extraction

The proposed segmentation was applied to the three hand databases mentioned above. To ensure the method's efficacy across all datasets, we selected hand images with specifically two fingers interlocked. The ROI extraction results for each are shown in Figures 9, 10, 11 and 12, for the contactless databases Tongji, GPDS, IITD and PolyUData, respectively.

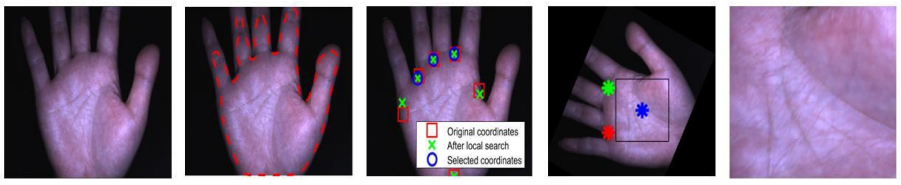

Figure 9. Tongji hand dataset ROI extraction: (a) Input image, (b) Active-contour segmentation, (c) Valley-point extraction, (d) Rotation and ROI computing, (e) Final ROI.

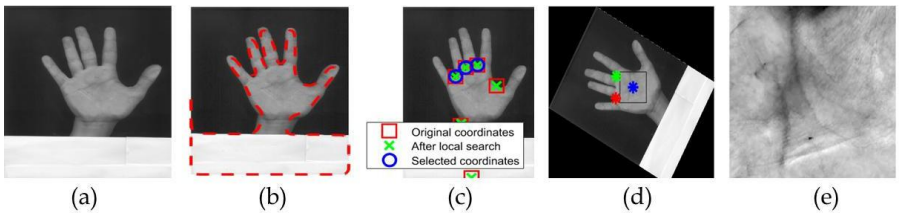

Figure 10. GPDS hand dataset ROI extraction: (a) Input image, (b) Active-contour segmentation, (c) Valley-point extraction, (d) Rotation and ROI computing, (e) Final ROI.

The proposed active-contour segmentation method offers a solution to the imprecise and low-quality results of previously used methods and works that use edge detectors and threshold methods for ROI extraction [45]. Figure 13 illustrates our proposed active-contour method performance in comparison with the threshold method. In 1, in the absence of active contours, with Otsu segmentation, the hand images with fingers poorly spread, resulting in incomplete contour (a). This leads to an error in valley

Jordanian Journal of Computers and Information Technology (JJCIT), Vol. 11, No. 04, December 2025.

positions, particularly those associated with the two fingers that are attached to the ring and middle fingers (b), these valley points serve as the basis to calculating the area's ROI. Therefore, it is impossible to determine the rectangle, and the final ROI cannot be extracted. In contrast, as shown in 2, by implementing our proposed segmentation, it allowed for extracting the entire contour, including that of the narrow region, successfully identifying all correct valley points, and finally extracting the yield ROI.

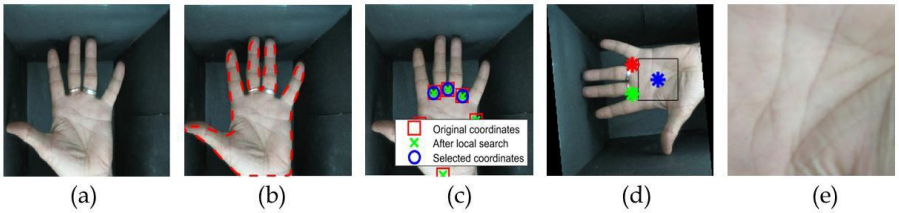

Figure 11. IITD hand dataset ROI extraction: (a) Input image, (b) Active-contour segmentation, (c) Valley-point extraction, (d) Rotation and ROI Computing, (e) Final ROI.

4.3 Palmprint Recognition

The training process is assessed using the Modified LOOCV. Initially, the three datasets are split into classes, with 10 samples of each class representing a person. For testing, two images are selected from each class, while using the remaining images for training. For instance, the GPDS dataset has 1,500 images divided into 150 classes. Leaving out two images per class for testing in the first iteration, a total of 300 images are used for testing data. Thus, the test set will contain 20% of the entire images and 80% in the training dataset, that holds for every other database.

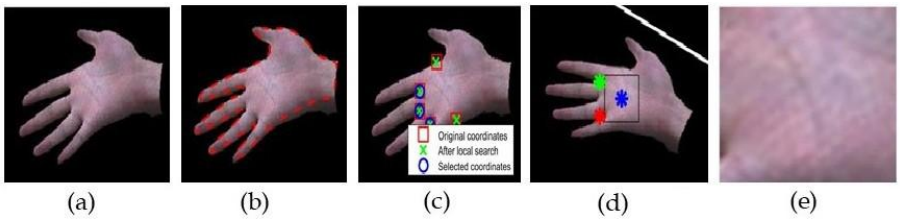

Figure 12. PolyU hand dataset ROI extraction: (a) Input image, (b) Active-contour segmentation, (c) Valley-point extraction, (d) Rotation and ROI computing, (e) Final ROI.

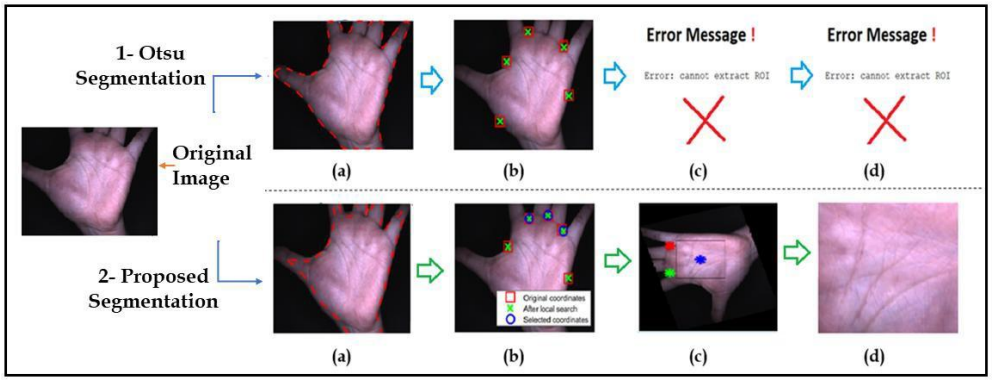

Figure 13. Active-contour performance for precise ROI extraction: (a) Segmentation, (b) Valley-point extraction, (c) Rotation and ROI computing, (d) Final ROI.

Our model was trained over 50, 100, and 200 epochs. When comparing the execution results, we found that the best accuracy and the fastest convergence rate were obtained within 100 epochs, with a learning rate of 10^{-5} for Tongi and IITD datasets, and 10^{-4} for the GPDS database. All metrics are evaluated once the first LOOCV iteration is completed by determining the average accuracy and the Equal Error Rate (EER), along with additional performance metrics, including Precision, Recall, and F1-score. Precision measures the proportion of correctly identified positive samples among all predicted positives, recall represents the proportion of correctly identified positive samples among all actual positives, and F1-score is the harmonic mean of precision and recall, reflecting the overall

balance between them. The applied model achieved the best accuracy of 99.75% on the Tongji dataset. Table 5 displays the accuracy, EER, precision, Recall, and F1-score results for the available datasets. The evaluation metrics obtained demonstrate that the model is well generalized. The high and balanced precision and recall values indicate that the model effectively identifies genuine matches while maintaining a low rate of false predictions. These findings validate that the model provides good discrimination ability across different datasets.

Table 5. Recognition performance on different datasets.

Dataset	Precision	EER	Accuracy (%)	Recall	F1-score
Tongji DB	0.9980	0.002	99.75%	0.9930	0.9955
IITD DB	0.9929	0.04	95.9 ± 1.0%	0.9461	0.9690
GPDS DB	0.9973	0.01	99.2%	0.9932	0.9952

The proposed palmprint-recognition system performs exceptionally well across three different databases according to ROC, accuracy and loss graphs illustrated in Figures 14, 15, 16 and 17. Approximate values showed an accuracy of about 99.75% in the Tongji database, 99.2% in GPDS dataset, and 95.9% in the IITD database. These accuracy values demonstrate how well the system can recognize palmprint images, demonstrating its excellent efficacy in handling a wide range of data. Turning to the loss, the results remained extremely low, suggesting that the model learns effectively and minimizes errors during the training process.

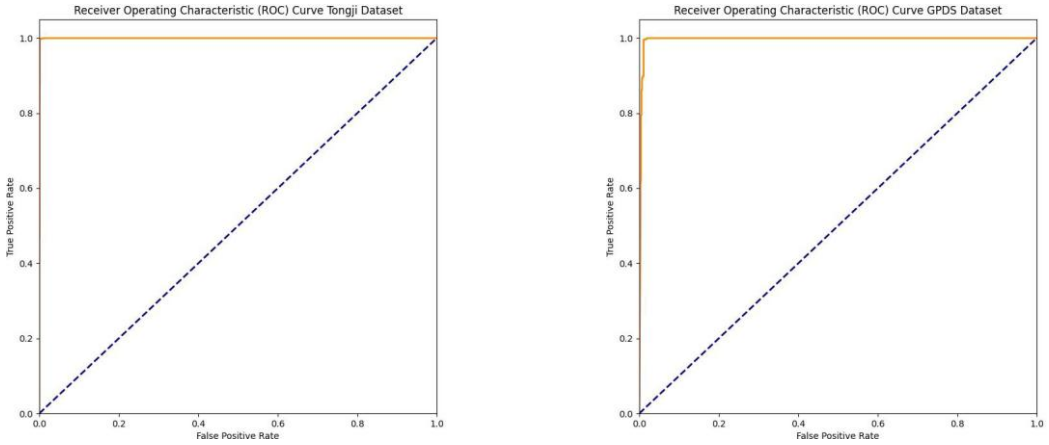

(a)ROC curve for the Tongji dataset (b) ROC curve for the GPDS dataset

Figure 14. Receiver operating characteristic (ROC) curves.

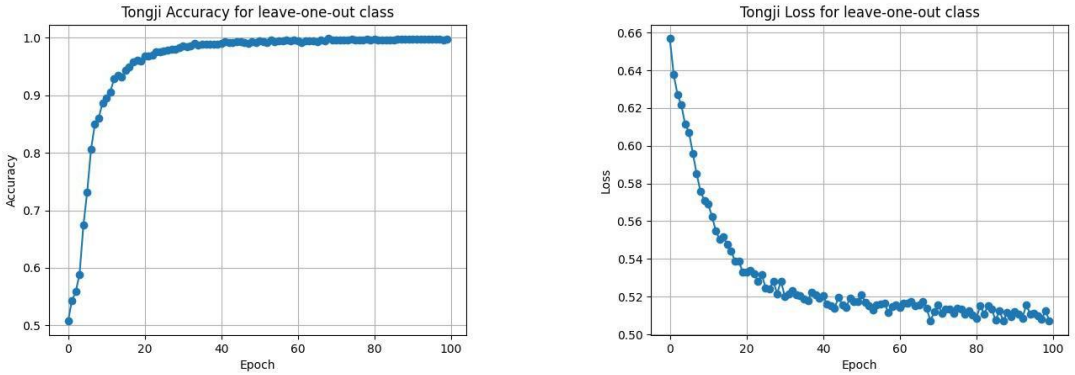

(a) Accuracy on Tongji dataset (b) Loss on Tongji dataset

Figure 15. Test-accuracy and loss curves for Tongji dataset.

Analyzing Table 5, the Tongji dataset exhibits the highest performance among the datasets, with the lowest EER of 0.002, indicating the most precise and well-balanced trade-off. While the GPDS dataset offers a slightly better EER than the IITD dataset, it nevertheless offers insightful performance. Overall, these findings demonstrate the high level of recognition accuracy of our system-based

palmprints over several datasets. The plots of ROC curves for the three available databases are displayed in Figure 14 for Tongji and GPDS datasets, and in Figure 17 for the IITD data, for a more thorough explanation and confirmation of our system's performance. These curves plot the True Positive Rate against the False Positive Rate. Completing our model execution, the AUC values were converging to 1 for both Tongji and GPDS, and to 0.97 for the IITD dataset. Regarding distinguishing between positive and negative classes, the Tongji dataset demonstrates the highest AUC, indicating nearly perfect performance. The high AUC values for the other datasets also indicate strong model performance. This generalization demonstrates the stability and high recognition accuracy of the Modified LOOCV-based Siamese network across a variety of datasets. Our approach proved its efficacy compared to recent related works, as illustrated in Table 6.

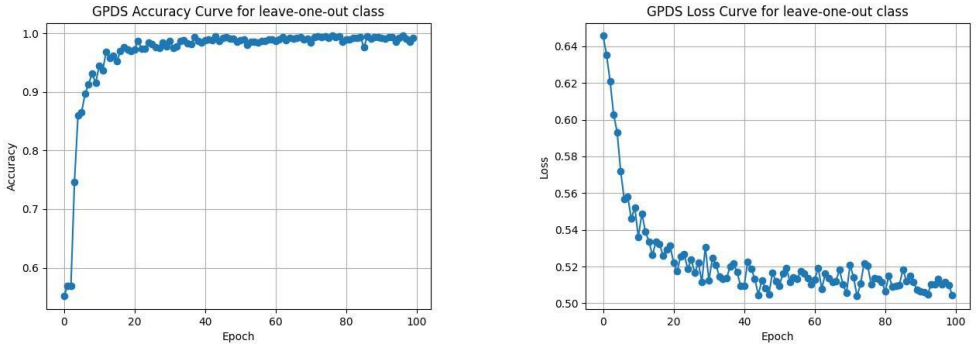

(a) Accuracy on GPDS dataset (b) Loss on GPDS dataset

Figure 16. Test accuracy and loss curves for GPDS dataset.

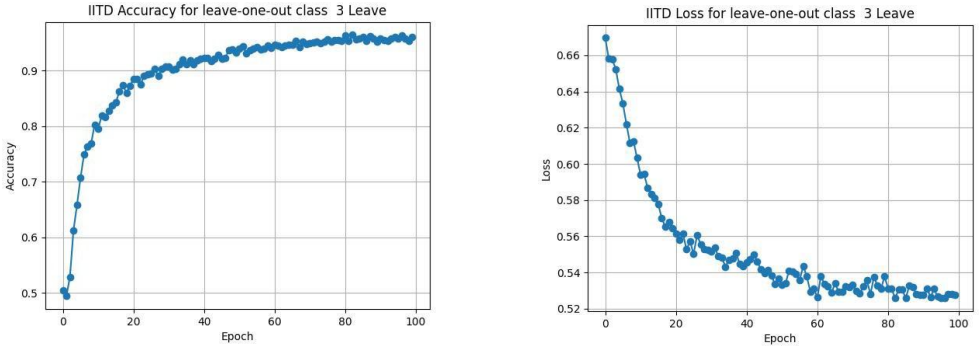

(a) Accuracy on IITD dataset (b) Loss on IITD dataset

Figure 17. Test-accuracy and loss curves for IITD dataset.

Table 6. Comparative accuracy performance of the proposed method relative to similar works. Accuracy (%) and EER (decimal).

Ref./Method	**IITD**	**Tongji**	**GPDS**
[46] HOG-SGF-AE	-	98.85%	-
[47] MTCC	EER=3.94	EER=0.0043	-
[48] MTPSR	-	-	96.83%
[49] DeepNet/ResNet	95.5%	99.5%	-
[50] SMHNet	-	97.36%	-
[51] Meta Metric Learning	94.02%	93.39%	-
[23] Transformer-GLGAnet	–	98.5%	-
[52] CCNet	EER=0.0018	EER=0.00004	-
[53] CO^{3}Net	EER=0.0047	EER=0.0050	-
[21] FedML (Triplet)	89.13% EER=0.0569	93.51% EER=0.0296	-
[54] **Siamese Net**	94.3%	97.7%	-
Ours	**95.9%** **EER=0.04**	**99.75%** - **EER=0.002**	**99.2%** - **EER=0.01**

In order to reinforce the previous findings and demonstrate the efficacy of our proposed Modified-LOOCV with the Siamese network, we trained the Siamese model with a random split of the database without applying the proposed LOOCV. The results confirmed the effectiveness of the Modified LOOCV in increasing the accuracy rate, where the accuracy was higher than that of the normal data splitting technique by 2.5%. The comparative analysis is shown in Figure 18; we adopted the IITD database results, since it demonstrated a significant transition, particularly in the ROC curve.

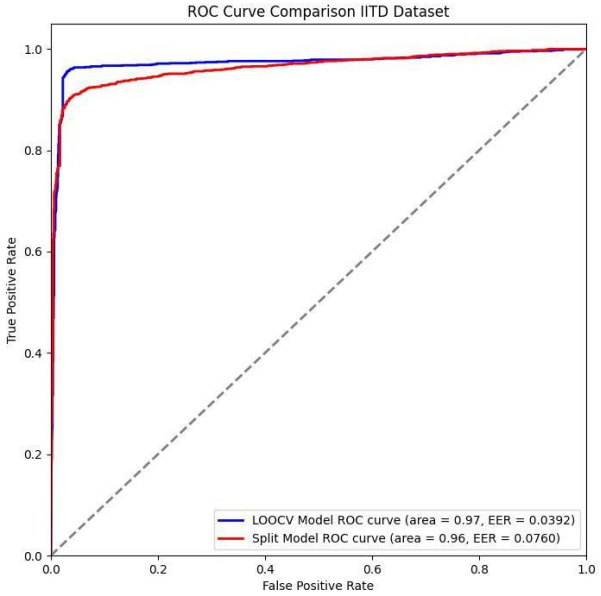

Figure 18. ROC-curve comparison: Modified-LOOCV *vs.* standard dataset split.

Table 7. Comparison of matching times for Tongji dataset.

Method	Matching time (ms)
VGG-16	26.8
PalmNet	22.8
Ours	**20**

In the prediction phase, we evaluated the precision and speed of the proposed Siamese network based on Modified LOOCV, by measuring the time needed to test and predict new images. It is important to note that the model was not trained on these test images previously. When compared to previous works' matching times, we obtain a matching time of 0.02 seconds (20 ms), where our model achieves a prediction speed that is competitive with widely adopted CNN-based palmprint recognition systems based on CNNs. Table 7 displays a brief comparison result with certain methods described in [49] on Tongji dataset.

The model compares two images and computes a similarity score to determine whether they belong to the same person. To interpret these scores, we applied Gradient-based SHapley Additive exPlanations (GradientSHAP) and Saliency Maps. GradientSHAP combines gradients with SHAP values to estimate feature contributions, while Saliency Maps identify the regions with the greatest influence on the output. As shown in Figures 19 and 20, both methods reveal that the network focuses on palmprint line structures. The Saliency Maps emphasize the most discriminative patterns, whereas GradientSHAP assigns importance across ridges and creases. These visual explanations demonstrate that the network depends on significant palmprint traits rather than on irrelevant background.

A further test was performed using various palmprint images from available databases, two types of test were performed. The first used images from the trained datasets, where a few images were excluded before training and placed in a separate folder for prediction. This ensured that these samples were never seen by the network during the training process. The obtained results on the GPDS dataset in Figure 19 show that the model accurately recognized these unseen samples with high similarity scores. The second test was conducted using images from the PolyU dataset, as shown in Figure 20, which were entirely unseen by the network. The model also achieved very good similarity results on this external dataset, confirming its strong generalization ability.

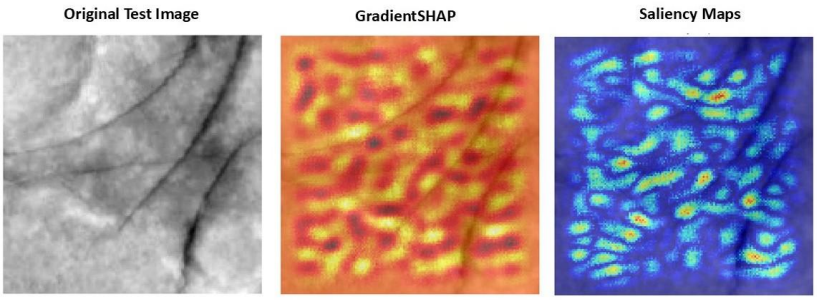

(a) Interpretability of palmprint similarity predictions.

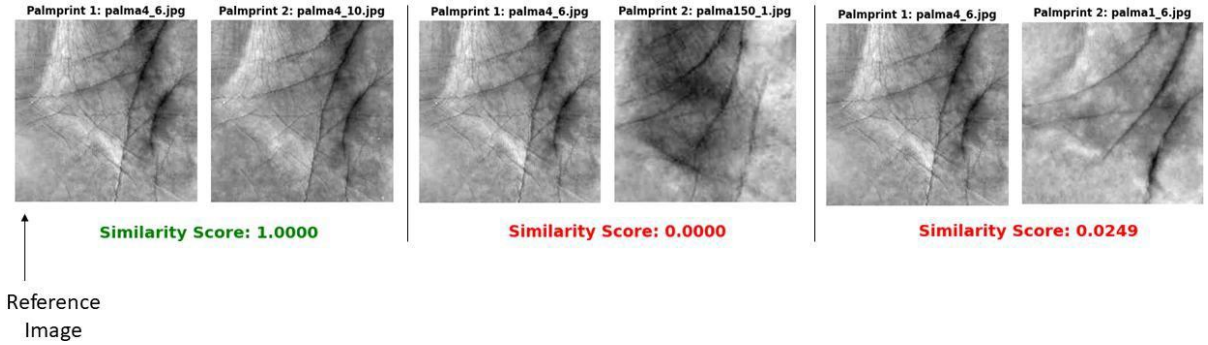

(b) Similarity-score prediction.

Figure 19. GPDS palmprint verification.

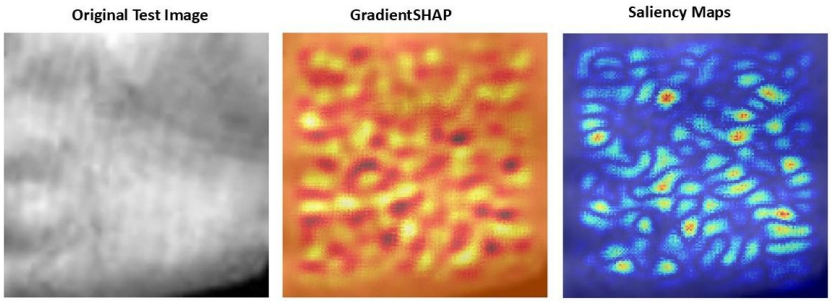

(a) Interpretability of palmprint similarity predictions.

(b) Similarity score prediction.

Figure 20. PolyU palmprint verification.

The system verifies that the two images are not of the same person when the score is less than the threshold value and *vice versa*. We chose a threshold of 0.5, which is adjustable based on the needs of the security system. We compared a reference image with three other images of three different random individuals. As illustrated in Figures 19 and 20, the model assigns a score close to 1.0 for palmprints belonging to the same individual, while the score approaches 0.0 for palmprints from different individuals. The attribution results highlight the palmprint regions that most influenced the predictions, with both methods consistently focusing on principal palm lines, ridge intersections and local ridge textures. Such interpretability increases security when using the model for real-world applications and makes the model's decisions more transparent.

5. CONCLUSION

A palmprint-recognition system based on deep learning has been developed, providing a highly efficient technique to predict palmprints by integrating a Modified-LOOCV strategy with a flexible Siamese architecture. To ensure a thorough assessment and model optimization, we initially provide an ROI-extraction technique based on active-contour segmentation. This approach can extract the ROI with variable contrasts and with excellent precision. The proposed Modified-LOOCV is an innovative strategy designed for datasets with significant sample similarity. We effectively capture the wide variety of the dataset while reducing computational time and enhancing the standard Siamese network efficacy. This enhancement enables the fast evaluation of the model's performance, providing an indication of its power and supporting its quick integration into real-world applications, such as access control and forensic identification, with high accuracy and low computational cost. The proposed model reaches an accuracy of up to 99.75%; it is competitive with many existing systems due to its accuracy and execution speed, even on small databases. The findings demonstrate that the suggested model has the potential to be widely used in real-world biometric identification systems, as it can efficiently learn discriminative palmprint characteristics and retain strong recognition performance even when evaluated on unseen data. In future work, we intend to extend and apply the proposed scheme to the Multi-Spectral Palmprint dataset and further generalize the methodology for diverse pattern-recognition systems to provide a deeper validation of its adaptability, robustness and applicability.

ACKNOWLEDGEMENTS

This work has been partially funded by the Spanish Government-Agencia Estatal de Investigacion-through projects´ PID2020-115220RB-C22 and PID2021-128009OB-C33, in collaboration with the Signals and Images Laboratory (LSI) at the University of Oran, USTO-MB, Algeria.

REFERENCES

[1] S. Dargan and M. Kumar, "A Comprehensive Survey on Biometric Recognition Systems Based on Physiological and Behavioral Modalities," Expert Systems with Applications, vol. 143, p. 113114, 2020.

[2] A. Genovese, V. Piuri and F. Scotti, Touchless Palmprint Recognition Systems, Part of the Book Series: Advances in Information Security (ADIS), vol. 60, Springer, 2014.

[3] A. Serrano, I. M. de Diego, C. Conde and E. Cabello, "Recent Advances in Face Biometrics with Gabor Wavelets: A Review," Pattern Recognition Letters, vol. 31, no. 5, pp. 372–381, 2010.

[4] J. Qian, J. Yang, Y. Tai and H. Zheng, "Exploring Deep Gradient Information for Biometric Image Feature Representation," Neurocomputing, vol. 213, pp. 162–171, 2016.

[5] A. Vinay, C. A. Kumar, G. R. Shenoy, K. N. B. Murthy and S. Natarajan, "ORB-PCA Based Feature Extraction Technique for Face Recognition," Procedia Computer Science, vol. 58, pp. 614–621, 2015.

[6] R. Yadav, S. K. Singh and R. Yogi, "Biometric Network Security Enhancements through Deep Learning Techniques," Proc. of the 2023 IEEE Int. Conf. on ICT in Business Industry & Government (ICTBIG), pp. 1–6, Indore, India, 2023.

[7] S. Minaee, A. Abdolrashidi, H. Su, M. Bennamoun and D. Zhang, "Biometrics Recognition Using Deep Learning: A Survey," Artificial Intelligence Review, vol. 56, no. 8, pp. 8647–8695, 2023.

[8] H. Heidari and A. Chalechale, "Biometric Authentication Using Deep Learning Based on Multi-level Fusion of Finger-knuckle Print and Fingernail," Expert Systems with Appl., vol. 191, p. 116278, 2022.

[9] D. Zhong, X. Du and K. Zhong, "Decade Progress of Palmprint Recognition: A Brief Survey," Neurocomputing, vol. 328, pp. 16–28, 2019.

[10] S. Joshi, D. K. Verma, G. Saxena and A. Paraye, "Issues in Training Convolutional Neural Networks for Image Classification," Proc. of Advances in Computing and Data Sciences (ICACDS 2019), Part of the Book Series: Comm. in Computer and Information Science (CCIS), vol. 1046, pp. 282–293, 2019.

[11] Y. Wang, J. Li, M. Zhang and G. Xu, "Palm Vein Recognition in Few-shot Learning *via* Modified Siamese Network," Proc. of the 2024 4th Int. Conf. on Neural Networks, Information and Communication Engineering (NNICE), pp. 598–603, Guangzhou, China, 2024.

[12] N. Elaraby, S. Barakat and A. Rezk, "A Novel Siamese Network for Few/Zero-shot Handwritten Character Recognition," Computers, Materials & Continua, vol. 74, no. 1, pp. 1837-1854, 2023.

[13] A. Hussain, A. Ullah, A. Aslam and A. Khatoon, "A Modified Siamese Network for Facial Assimilation," WSEAS Transactions on Signal Processing, vol. 19, pp. 60–66, 2023.

[14] A. Singh, A. Kumar and S. Lukose, "Forensic Acoustic Applications of Siamese Neural Networks,"

Proc. of the 2024 3rd Int. Conf. for Innovation in Technology (INOCON), pp. 1–4, 2024.

[15] C. R. Kumar et al., "Face Recognition Using CNN and Siamese Network," Measurement: Sensors, vol. 27, p. 100800, 2023.

[16] E. AlShemmary and F. A. Ameen, "Siamese Network-based Palmprint Recognition," Journal of Kufa for Mathematics and Computer, vol. 10, no. 1, pp. 108–118, 2023.

[17] D. M. Aprilla et al., "Palmprint Recognition Using Xception, VGG16, ResNet50, MobileNet and EfficientNetB0," J. Media Inform, Budidarma, vol. 8, no. 2, pp. 1065–1076, 2024.

[18] F. Liao, F. Leng, Z. Yang and B. Zhang, "Multi-order Extension Codes for Palmprint Recognition," International Journal of Neural Systems, vol. 35, no. 8, p. 2550039, 2025.

[19] L. Yan, F. Wang, F. Leng and A. B. J. Teoh, "Toward Comprehensive and Effective Palmprint Reconstruction Attack," Pattern Recognition, vol. 155, p. 110655, 2024.

[20] H. Shao, S. Shi, X. Du, D. Zeng and D. Zhong, "Robust Palmprint Recognition *via* Multi-stage Noisy Label Selection and Correction," IEEE Trans. on Image Processing, vol. 34, pp. 4591– 4601, 2025.

[21] H. Shao, C. Liu, C. Li and D. Zhong, "Privacy-preserving Palmprint Recognition *via* Federated Metric Learning," IEEE Transactions on Information Forensics and Security, vol. 19, pp. 878–891, 2023.

[22] H. Shao, Y. Zou, C. Liu, Q. Guo and D. Zhong, "Learning to Generalize Unseen Dataset for Cross-dataset Palmprint Recognition," IEEE Trans. on Inf. Forensics and Secu., vol. 19, pp. 3788–3799, 2024.

[23] K. Zhang et al., "Palmprint Recognition Based on Gating Mechanism and Adaptive Feature Fusion," Frontiers in Neurorobotics, vol. 17, p. 1203962, 2023.

[24] J. Q. Du et al., "Advancements in Image Recognition: A Siamese Network Approach," Information Dynamics and Applications, vol. 3, no. 2, pp. 89–103, 2024.

[25] F. Marattukalam et al., "N-shot Palm Vein Verification Using Siamese Networks," Proc. of the 2021 IEEE Int. Conf. of the Biometrics Special Interest Group, pp. 1–5, Darmstadt, Germany, 2021.

[26] V. Gurunathan et al., "Palm Vein Biometric System Using Siamese Neural Network," Proc. of the 2024 IEEE Int. Conf. on Science Technology Eng. and Manag. (ICSTEM), pp. 1–5, Coimbatore, India, 2024.

[27] D. Zhong, Y. Yang and X. Du, "Palmprint Recognition Using Siamese Network," Proc. of the 13th Chinese Conf. (CCBR 2018), pp. 48–55, DOI: 10.1007/978-3-319-97909-0_6, Urumqi, China, 2018.

[28] X. Du, D. Zhong and P. Li, "Low-shot Palmprint Recognition Based on Meta-Siamese Network," Proc. of the 2019 IEEE Int. Conf. on Multimedia and Expo (ICME), pp. 79–84, Shanghai, China, 2019.

[29] H. Shao et al., "Few-shot Learning for Palmprint Recognition *via* Meta-Siamese Network," IEEE Transactions on Instrumentation and Measurement, vol. 70, p. 5009812, 2021.

[30] C. Liu et al., "Siamese-hashing Network for Few-shot Palmprint Recognition," Proc. of the 2019 IEEE Symposium Series on Computational Intelligence (SSCI), pp. 3251–3258, Xiamen, China, 2019.

[31] S. Younus et al., "Palmprint Recognition Using Deep Convolutional Neural Networks," Proc. of the 2022 IEEE 2nd Int. Maghreb Meeting of the Conf. on Sciences and Techniques of Automatic Control and Computer Engineering (MI-STA), pp. 539–543, Sabratha, Libya, 2022.

[32] W. M. Cherif et al., "Active Contour Segmentation and CNN for Palmprint Recognition," Proc. of the 2022 2nd Int. Conf. on New Techn. of Inf. and Comm. (NTIC), pp. 1–6, Mila, Algeria, 2022.

[33] M. Ezz et al., "Improved Siamese Palmprint Authentication Using Pre-trained VGG16-palmprint," Computer Systems Science & Engineering, vol. 46, no. 2, pp. 2299-2317, 2023.

[34] R. Chen et al., "Research on Palmprint Recognition Based on Mechanism and Data," Proceedings of the Int. Conf. on Computer Vision and Deep Learning (CVDL'24), Article no. 66, pp. 1–9, DOI: 10.1145/3653804.3656264, 2024.

[35] A. A. Amini et al., "Using Dynamic Programming for Minimizing the Energy of Active Contours with Hard Constraints," Proc. of the 2nd Int. Conf. on Computer Vision, pp. 95–99, Tampa, USA, 1988.

[36] K. Ito et al., "Palm Region Extraction for Contactless Palmprint Recognition," Proc. of the 2015 IEEE Int. Conf. on Biometrics (ICB), pp. 334–340, Phuket, Thailand, 2015.

[37] T. Connie et al., "Automated Palmprint Recognition System," Image and Vision Computing, vol. 23, no. 5, pp. 501–515, 2005.

[38] V. W. Lumumba, "Comparative Analysis of Cross-validation Techniques: LOOCV, K-fold and Repeated K-fold in Machine Learning Models," American J. of Theoretical and Applied Statistics, vol. 13, no. 5, pp. 127-137, 2024.

[39] Zhang, Lin: "Contactless Palmprint Database," [Online], Available: https://cslinzhang.github.io/ ContactlessPalm/, Accessed: July 11, 2025.

[40] L. Zhang et al., "Towards Contactless Palmprint Recognition: A Novel Device, New Benchmark and Collaborative Representation Approach," Pattern Recognition, vol. 69, pp. 199–212, 2017.

[41] IIT Delhi Biometric Database, IIT Delhi Touchless Palmprint Database, [Online], Available: https://www4. comp.polyu.edu.hk/~csajaykr/IITD/Database_Palm.htm, Accessed: Sep. 1, 2024.

[42] A. Kumar, "Incorporating Cohort Information for Reliable Palmprint Authentication," Proc. of the 2008 IEEE 6th Indian Conf. on Computer Vision, Graphics & Image Processing (ICVGIP), pp. 583–590, Bhubaneswar, India, 2008.

[43] M. A. Ferrer et al., "Low-cost Multi-modal Biometric Identification Based on Hand Geometry and Texture," Proc. of the 2007 41st Annual IEEE Int. Carnahan Conf. on Security Technology, pp. 52–58,

Ottawa, Canada, 2007.
[44] V. Kanhangad, A. Kumar and D. Zhang, "Contactless and Pose-invariant Biometric Identification Using Hand Surface," IEEE Transactions on Image Processing, vol. 20, no. 5, pp. 1415–1424, 2010.
[45] D. Zhang, W. K. Kong, J. You and M. Wong, "Online Palmprint Identification," IEEE Transactions on Pattern Analysis and Machine Intelligence, vol. 25, no. 9, pp. 1041–1050, 2003.
[46] A. Gumaei et al., "Effective Palmprint Recognition for Visible and Multi-spectral Images," Sensors, vol. 18, no. 5, p. 1575, 2018.
[47] Z. Yang et al., "Multi-order Texture Features for Palmprint Recognition," Artificial Intelligence Review, vol. 56, no. 2, pp. 995–1011, 2023.
[48] L. Liang, T. Chen and L. Fei, "Orientation Space Code and Multi-feature Two-phase Sparse Representation for Palmprint Recognition," Int. Journal of Machine Learning and Cybernetics, vol. 11, pp. 1453–1461, 2020.
[49] T. Chai, S. Prasad and S. Wang, "Boosting Palmprint Identification with Gender Information Using DeepNet," Future Generation Computer Systems, vol. 99, pp. 41–53, 2019.
[50] C. Liu, D. Zhong and H. Shao, "Few-shot Palmprint Recognition Based on Similarity Metric Hashing Network," Neurocomputing, vol. 456, pp. 540–549, 2021.
[51] H. Shao and D. Zhong, "Towards Open-set Touchless Palmprint Recognition *via* Weight-based Meta Metric Learning," Pattern Recognition, vol. 121, p. 108247, 2022.
[52] Z. Yang et al., "Comprehensive Competition Mechanism in Palmprint Recognition," IEEE Transactions on Information Forensics and Security, vol. 18, pp. 5160–5170, 2023.
[53] Z. Yang et al., "CO3Net: Coordinate-aware Contrastive Competitive Neural Network for Palmprint Recognition," IEEE Transactions on Instrumentation and Measurement, vol. 72, pp. 1–14, 2023.
[54] A. Fawzy, M. Ezz, S. Nouh and G. Tharwat, "Palmprint Recognition Using Siamese Network and Transfer Learning," International Journal of Advanced and Applied Sciences, vol. 9, no. 3, pp. 90–99, 2022.

ملخص البحث:

إنّ التّقدُّم في انظمة التّعلُّم العميق البيومترية، التي طُبّقت فيها طرق تمييز الأشخاص عن طريق الوجه واليد، يقود إلى تحسيناتٍ من حيث الأداء السّريع و سرّية البيانات. وإنّ التّعرُّف على بصمات الكف هو الموضوع الرّئيسي الّذي يتمّ التّركيز عليه في الطّريقة المقترحة في هذه الورقة، حيث يتمّ التّعامل مع مجموعات بياناتٍ أصغر حجماً من غيرها من مجموعات البيانات البيومترية. وتجدر الإشارة إلى أنّ نموذجاً ضخماً ومعقّداً من أنظمة التّعلُّم العميق قد يخسر شيئاً من مواءمته وقدرته على التّعميم عندما يُطبّق على هذا النّوع من البيانات.

تعالج هذه الورقة التّحدّيات آنفة الذّكر عن طريق تطبيق نموذج تعلُّم عميق ملائم للتّعرُّف على بصمات الكف الّتي تتميز بالتّنوُّع ومحدودية البيانات. في بادىء الأمر، يتمّ استخلاص "منطقة الاهتمام" باستخدام التّجزئة النّشطة الّتي تناسب التّعامل مع صعوبة الحصول على بصمات الكف من صُور اليد الّتي تحتوي على أصابع مُتقاربة أو متلاصقة. أمّا في المرحلة الثانية، فتُستخدم طريقة جديدة ومخصّصة مدفوعة بطريقة (LOOCV) بعد تعديلها ودمجها بشبكة تعلُّم عميقٍ سياميةٍ للتّحقُّق من بصمات الكف. وعلى النّقيض من طريقة (LOOCV) التّقليدية، فإنّ طريقتنا المعدّلة تعمل على تحسين الكلفة الحسابية في الوقت الّذي يتمّ فيه الحصول على تقييمٍ متوازنٍ على ثلاث مجموعات بيانات.

ويعمل إطار العمل المقترح على إثبات فاعلية أنظمة التّعرُّف على بصمات الكف الّتي تستخدم تقنياتٍ متقدّمة؛ فقد تمّ تحقيق دقّة مقدارها 99.75% في التّعرُّف على الأشخاص عبر بصمات كفوفهم، إلى جانب تحسين (تقليل) معدّل خطأ التساوي وتسريع زمن المطابقة، الأمر الذي يجعل النّموذج المقترح ملائماً للتّطبيقات الميدانية.